

Mathematical and Computer Modelling of the Influence of Stress on Magnetic Characteristics of the Construction Steels

DOROTA JACKIEWICZ^a, ROMAN SZEWCZYK^b, JACEK SALACH^c

^a Industrial Research Institute for Automation and Measurements
Jerozolimskie 202, Warsaw, Poland
d.jackiewicz@mchtr.pw.edu.pl

^b Industrial Research Institute for Automation and Measurements
Jerozolimskie 202, Warsaw, Poland
rszewczyk@onet.pl

^c Institute of Metrology and Biomedical Engineering, Warsaw University of Technology
Boboli 8, Warsaw, Poland
j.salach@mchtr.pw.edu.pl

Received 20 October 2012, Revised 9 April 2013, Accepted 7 March 2013

Abstract: This paper concerns the possibility of use the Jiles-Atherton extended model to describe the magnetic characteristics of construction steel St3 under mechanical stress. Results of the modelling utilizing extended Jiles-Atherton model are consistent with results of experimental measurements for magnetic hysteresis loops B(H). Material stress state determination by using non-destructive, magnetic properties based on testing techniques is an especially important problem.

Keywords: construction steel, magnetic characteristics modelling, non-destructive testing, stress influence

1. Introduction

Magnetic method is often used in non-destructive testing of ferromagnetic elements of constructions. The most important inconvenience of this method is its limitation only to the comparative measurements. For this reason, it is important to develop the material's magnetisation model, which will enable a generalised description of the characteristics of magnetisation changes and only accordingly to the mechanical state of that material. This model should be based on physical principles, and to comprise the influence of mechanical stress or fatigue failures.

Among many models of magnetisation of ferromagnetic materials, used in non-destructive testing of construction steel, the Jiles-Atherton model [1] appears to be the most useful. This model not only reproduces mathematically the magnetic hysteresis loops, but also takes into account the physical aspect of the material magnetisation process. For this reason, it is used in stress assessment of ferromagnetic construction materials and is widely documented in literature.

However, Jiles-Atherton model has significant limitations. For one set of calculated model parameters, the results of the modelling are in correspondence with the results of experimental measurements, but only for one of the amplitudes of the magnetising field.

Therefore, in these studies the Jiles-Atherton extended model is used [2], which allows to avoid this disadvantage. In all models based on Jiles-Atherton approach, model parameters are determined on the base of least squares, between the hysteresis loop obtained by modelling, and the hysteresis loop resulting from experimental measurements. However, for extended Jiles-Atherton model of magnetic characteristics, the determination of model's parameters on the base of commonly used gradient optimisation is not successful, due to the presence of local minima. For this reason the evolutionary strategies were proposed.

The paper presents a novel method of determination of the Jiles-Atherton model parameters. The method can enable technological breakthrough in non-destructive testing of construction steels and can be used to monitor state of stress of a building construction.

2. Jiles-Atherton model and its extension

The manuscript should be logically divided into sections. The body of the paper consists of numbered sections that present the main findings. Each sections should be preceded by numbered heading. As a heading the "subtitle" style should be used (Times New Roman, 11 points, bold). The analysis of the thermodynamic potentials is the basis of the Jiles-Atherton model [3]. These potentials characterise the thermodynamic transformations and are given by the following equations:

$$A = G + \mu_0 \cdot H \cdot M \quad (1)$$

$$G = U - T \cdot S + \frac{3}{2} \sigma \cdot \lambda \quad (2)$$

$$U = \frac{1}{2} \alpha \cdot \mu_0 \cdot M^2 \quad (3)$$

where: A is Helmholtz free energy, G is Gibbs free energy, U is materials internal energy, S is materials free entropy, M is magnetisation, H is magnetising field, $\mu_0 = 4\pi \cdot 10^{-7}$ H/m is vacuum permeability, T is materials temperature, σ is stress mechanics in material, λ is magnetostrictive strain and α is coefficient describing the coupling between the domain.

The magnetisation M in Jiles-Atherton model is given by the following equation:

$$M = M_{rev} + M_{irr} \quad (4)$$

where M is the sum of reversible magnetisation M_{rev} [4] and irreversible magnetisation M_{irr} represents the energy losses due to domain wall motion [4]. These quantities are represented by the following equations:

$$M_{rev} = c(M_{an} - M_{irr}) \quad (5)$$

$$\frac{dM_{irr}}{dH} = \delta_M \frac{M_{an} - M_{irr}}{\delta \cdot k} \quad (6)$$

where M_{an} is the anhysteretic magnetisation, c describes magnetization reversibility, parameter δ describes the sign of $\frac{dH}{dt}$, k quantifies average energy required to break pinning site and δ_M guarantees the avoidance of unphysical stages of the Jiles-Atherton model for minor loops, in which incremental susceptibility becomes negative.

The M_{an} anhysteretic magnetisation should be calculated from the equation [5]:

$$M_{an} = tM_{aniso} + (1-t)M_{iso} \quad (7)$$

where: t is weight coefficient, describing participation of anisotropic phase in the material M_{aniso} is anisotropic magnetisation and M_{iso} is isotropic magnetisation.

Isotropic magnetisation M_{iso} is given by the following equation [6]:

$$M_{iso} = M_s \left[\text{cath} \left(\frac{H_{eff}}{a} \right) - \left(\frac{a}{H_{eff}} \right) \right] \quad (8)$$

where $H_{eff} = H + \alpha M$ is effective magnetising field and a quantifies the domain of walls density.

Anisotropic magnetisation M_{aniso} in material is given by the equation [7]:

$$M_{aniso} = M_s \frac{\int_0^\pi e^{E(1)+E(2)} \sin \theta \cos \theta d\theta}{\int_0^\pi e^{E(1)+E(2)} \sin \theta d\theta} \quad (9)$$

where $E(1)$ and $E(2)$ are energies and are given by the equations [7]:

$$E(1) = \frac{H_{eff}}{a} \cos \theta - \frac{K_{an}}{M_s \mu_0 a} \sin^2(\psi - \theta) \quad (10)$$

$$E(2) = \frac{H_{eff}}{a} \cos \theta - \frac{K_{an}}{M_s \mu_0 a} \sin^2(\psi + \theta) \quad (11)$$

where K_{an} is an anisotropic energy density, ψ is an angle between the easy axis of the material and the magnetising field direction.

The original Jiles-Atherton model of magnetisation process utilizes seven parameters [4]: a – quantifies domain walls density, k – quantifies average energy required to break pinning site, c – coupling coefficient, α is inter domain coupling, K_{an} – anisotropy energy density, t – participation of anisotropic phase and M_s – saturation magnetisation. Equation for the anisotropic magnetisation can be calculated only by numerical methods, because there are no primary functions of the integral functions.

In the original model Jiles-Atherton it is assumed that the model parameters are constant in the whole range of magnetizing field H . This assumption greatly simplifies the model calculations. However, it is questionable from a physical point of view.

Nevertheless, extensions of the Jiles-Atherton model for isotropic materials, in which the chosen model parameters change as a function of the magnetizing field known from the literature, have no physical reasons. Description of the k parameter should correspond with the physical condition of the material, because this condition describes the value of the magnetization M in the material, not the value of the magnetizing field H . To achieve this, parameter k should be presented as a function of the magnetization M [2, 11]:

$$k = k_0 + \frac{e^{k_2 \cdot (1-|M|/M_s)} - 1}{e^{k_2} - 1} \cdot (k_1 - k_0) \quad (12)$$

where: k_0 determines the minimal value of k , k_1 parameter determines maximal value of k and k_2 is a shape parameter.

Parameters of extended Jiles-Atherton model were determined during the optimization process using evolutionary strategies and gradient-oriented methods

[8]. In the first step, evolutionary strategies ($\mu + \lambda$) [9] were used, combined with simulated annealing. In the second step, the gradient optimisation for the 20 best results obtained after the first step was used. In evolutionary strategies the population of vectors consists of parameters of the Jiles-Atherton extended model. During this process, population of λ individuals (descendants) is created from the population of μ individuals (parents). Copies of μ randomly selected individuals are parents. Next, on the base of μ parents, the population of λ descendants is created randomly using the operators of mutation and crossover. Then, population of $\mu + \lambda$ individuals is created. This population is a combination of population of descendants and population of parents. The best μ individuals from a population $\mu + \lambda$ create the new population for the next iteration.

The optimization process bases on the minimization of the target function. This function was given by the following equation:

$$F = \sum_{i=1}^n (B_{J-A-S}(H_i) - B_{meas}(H_i))^2 \quad (13)$$

where: n is number of measurement points, $B_{J-A-S}(H_i)$ are results of the modelling and $B_{pom}(H_i)$ are results of the experimental measurements. Target function F , during the optimization process was calculated simultaneously for 3 hysteresis loops measured for different magnetizing fields.

Population of 900 vectors was used in optimization process. A group of 3 vectors (parent) were subjected to the crossover operator generated 12 vectors (descendants). Then the descendants vectors were subjected to the mutation. The distribution of value changes of the parameters during in the process of mutation was a normal distribution whose standard deviation was equal to 3% of the initial value of the modified parameter. Every iteration, in accordance with the simulated annealing, the standard deviation decreased by 5%.

3. Methodology of measurements

Experimental measurements of magnetic characteristics of construction steel were made for the frame-shaped sample [10], which was made of construction steel *St3*. The length of sample was 200 mm and each column had 8 mm. Thickness of the sample was 2 mm. Sample was subjected to thermal relaxation, to reduce the value of residual stresses generated during the steel production process. Parameters of this relaxation were as follows: heating up to 650°C for 1,2 h, annealing for 0,3 h at 650°C and cooling with speed 75°/h up to 500°C. The sample was wound by 188 turns magnetizing winding and 51 turns of measuring winding.

In Figure 1 experimental setup for measurements of $B(H)$ characteristics of frame-shaped samples and its dependence on stress is shown.

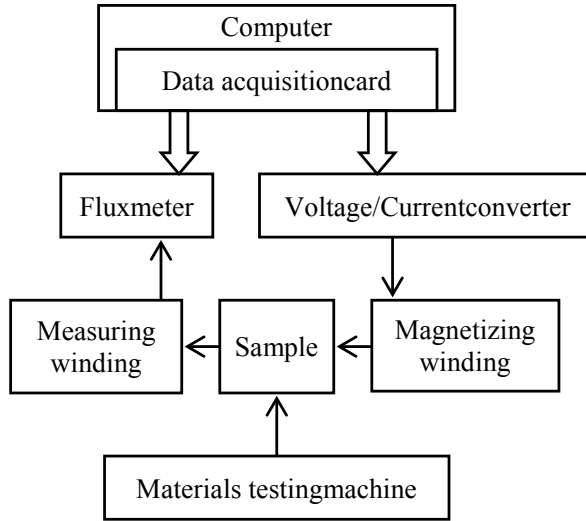


Fig. 1. Schematic block diagram of a measuring setup

The measuring setup is controlled by PC equipped with NI USB 6525 data acquisition card. This card is controlled by NI LabView software, which enables real-time control as well as data processing. Voltage sine wave generated by the data acquisition card drives voltage/current converted Kepco BOP 36. The output of Kepco BOP 36 is connected to the magnetizing winding of the investigated core. Measuring winding is connected with the Laleshore 480 fluxmeter, which measures flux density B in the sample. Voltage output of the fluxmeter is connected to the data acquisition card. As a result, developed hysteresis graph presents $B(H)$ hysteresis loops under digitally controlled values of amplitude of magnetizing field as well as for different frequencies and shapes of magnetizing signals.

During the magnetoelastic measurements, frame-shaped sample was located in MTS Bionix Servohydraulic Test Systems (Figure 2). The sample was stretched with tensile stress below the yield point, up to 150 MPa. The influence of stress on the shape of $B(H)$ hysteresis loop was measurement for amplitude of magnetizing field H_m equal to 65 A/m, 110 A/m and 315 A/m, frequency was 0,1 Hz.

Next, on the basis of measurements, magnetic hysteresis loops of *St3* steel were modelled with Jiles-Atherton extended model. The hysteresis loop could be modeled in full range of magnetizing field, because the modified parameter k changes as a function of magnetization M of the material.

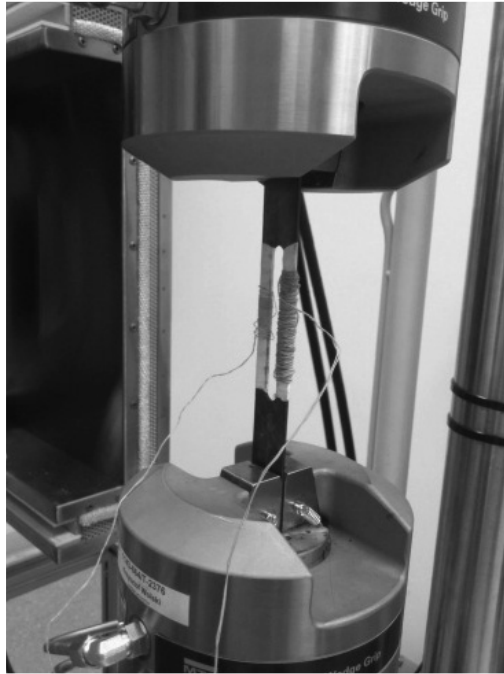


Fig. 2. Frame-shaped sample in MTS Bionix Servohydraulic during application of tensile stresses

4. Results

Figures 3, 4, 5 show the consistency between the results of modelling using Jiles-Atherton model and experimental results for *St3* steel. Each figure presents the results for the sample subjected to the three stresses: 0, 30, 150 MPa. Figures 3, 4, 5 show the results for magnetizing field H_m equal 65 A/m, 110 A/m and 315 A/m respectively. The experiment results confirm significant change of hysteresis loop shape under stresses. Results of the modelling utilising extended Jiles-Atherton model are consistent with results of experimental measurements which is confirmed by high values of the R^2 determination coefficient. The R^2 exceeds value of 99% for each of the magnetic hysteresis loop $B(H)$.

Figure 6 shows the changes in the values of the parameters of Jiles-Atherton model under the influence of increasing stresses. The value of saturation magnetisation M_s is constant with value of 599091 A/m. It is important, that one set of the parameters is sufficient to model the hysteresis loops over the whole magnetizing field amplitude from 65 A/m to 315 A/m, for a particular value of stress.

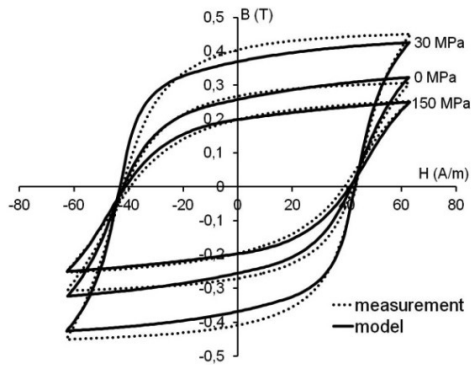


Fig. 3. The influence of tensile stresses on the shape of $B(H)$ hysteresis loops of St3 steel and the agreement between the results of modelling and experimental for $B(H)$ characteristics for magnetizing field 65 A/m

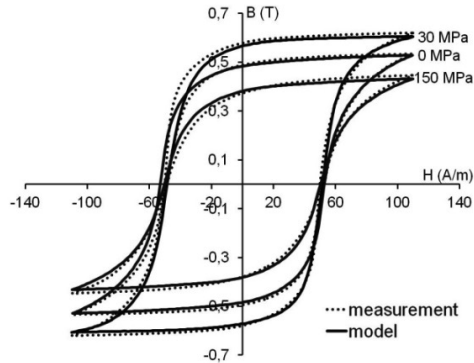


Fig. 4. The influence of tensile stresses on the shape of $B(H)$ hysteresis loops of St3 steel and the agreement between the results of modelling and experimental for $B(H)$ characteristics for magnetizing field 110 A/m

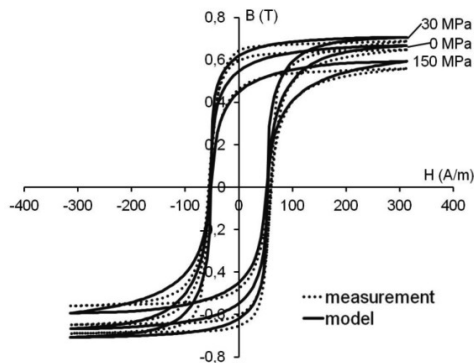


Fig. 5. The influence of tensile stresses on the shape of $B(H)$ hysteresis loops of St3 steel and the agreement between the results of modelling and experimental for $B(H)$ characteristics for magnetizing field 315 A/m

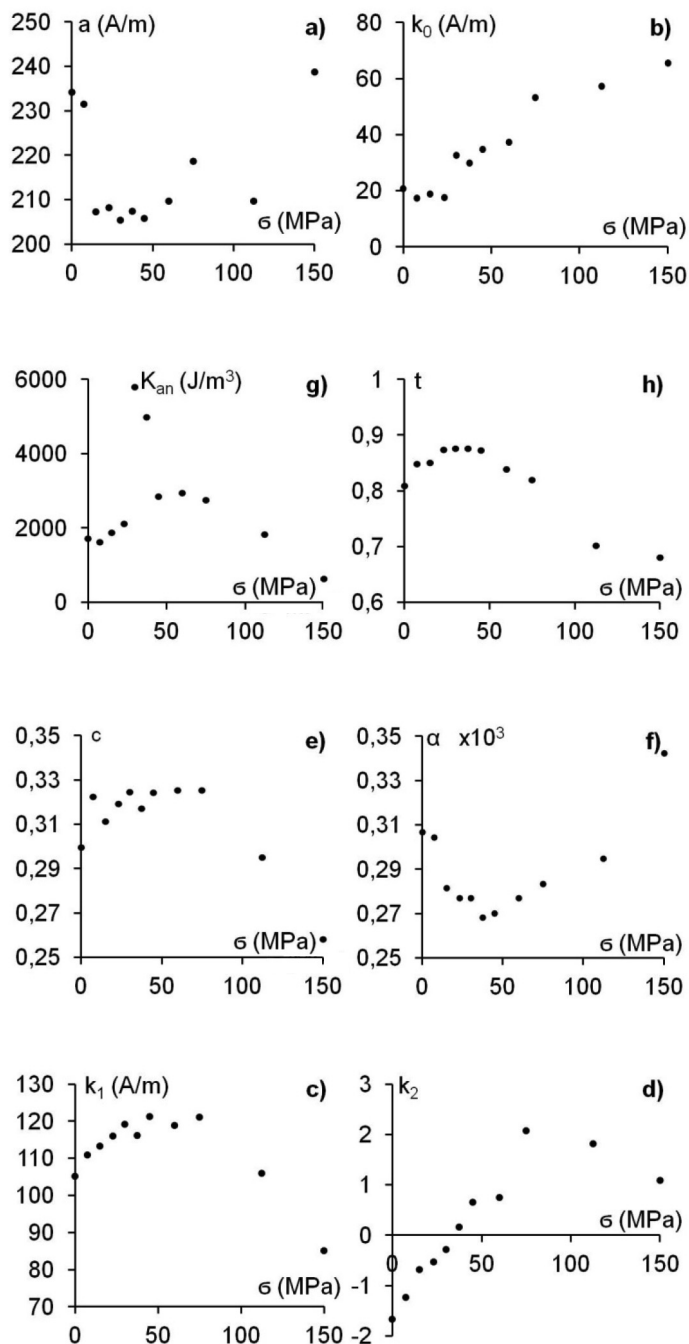


Fig. 6. The influence of tensile stresses σ on the parameters of extended Jiles-Atherton model

4. Conclusions

Results of the modelling utilizing extended Jiles-Atherton model are consistent with results of experimental measurements which is confirmed by high values of the R^2 determination coefficient. The results show correctness of proposed model for modelling of construction steel St3 under mechanical stress. Owing to the fact that in this modified model parameter k changes as a function of magnetization M of the material, the hysteresis loop could be modelled in full range of magnetizing field.

Presented results confirm that extended Jiles-Atherton model enables modelling the magnetic hysteresis loop with accuracy required for technical application. As a result, methodology presented in the paper may be the base for novel methods of estimation the level of stresses in the construction elements made of ferromagnetic steel.

References

1. M. J. Sablik, H. Kwun, G. L. Burkhardt, D. C. Jiles, *Model for the effect of tensile and compressive stress on ferromagnetic hysteresis*, J. Appl. Phys. 61, 1987, pp. 3799.
2. R. Szewczyk, *Extension for the model of the magnetic characteristics of anisotropic metallic glasses*, Journal of Physics D – Applied Physics 40, 2007, pp. 4109.
3. M. J. Sablik, G. L. Burkhardt, H. Kwun, D. C. Jiles, *A model for the effect of stress on the low-frequency harmonic content of the magnetic induction in ferromagnetic materials*, Journal of Applied Physics 63, 1988, pp. 3930.
4. D. C. Jiles, D. L. Atherton, *Ferromagnetic hysteresis*, IEEE Trans. Magn. 19, 1983, pp. 2183.
5. D. C. Jiles, A. Ramesh, Y. Shi, X. Fang, *Application of the anisotropic extension of the theory of hysteresis to the magnetization curves of crystalline and textured magnetic materials*, IEEE Trans. Magn. 33, 1997, pp. 3961.
6. D. C. Jiles, D. Atherton, *Theory of ferromagnetic hysteresis*, Journal of Magnetism and Magnetic Materials 61, 1986, pp. 48.
7. A. Ramesh, D. C. Jiles, J. Roderik, *A model of anisotropic anhysteretic magnetization*, IEEE Transactions on Magnetics 32, 1996, pp. 4234.
8. R. Szewczyk, *Modelling the magnetic and magnetostrictive properties of high permeability Mz-Zn ferrites*, Pramana – Journal of Physics 67, 2006, pp. 1165.
9. H. P. Schwefel, *Evolution and optimum seeking*, Wiley, New York, 1995.

10. A. Bieńkowski, *Some problems of measurement of magnetostriction in ferrites under stresses*, Journal of Magnetism and Magnetic Materials 112, 1992, pp. 143-145.
11. R. Szewczyk, *Modelling the magnetic characteristics of isotropic and anisotropic materials for sensor applications*, Acta Physica polonica A 113, 2008, pp. 67.

Matematyczne i komputerowe modelowanie wpływu naprężeń na charakterystyki magnetyczne stali konstrukcyjnej

Streszczenie

Niniejszy artykuł dotyczy możliwości wykorzystania rozszerzonego modelu Jilesa-Athertona do opisu wpływu naprężeń na charakterystyki magnetyczne stali konstrukcyjnej. Oryginalny model zakłada, że parametry modelu są stałe w całym zakresie pól magnesujących H . Zastosowane rozszerzenie pozwala modelować pętle histerezy dla różnych wartości pól magnetycznych. Jest to możliwe dzięki powiązaniu wartości parametru k mówiącom o średniej energii koniecznej do pokonania zaczepu ścian domenowych z magnetyzacją (zależność 12).

Do badań eksperymentalnych wykorzystano próbkę ramkową ze stali St3. Na rysunku 1 przedstawiono układ użyty do wytworzenia pola magnetycznego i pomiaru indukcji magnetycznej. Badaną próbkę poddana naprężeniom rozciągającym poniżej granicy sprężystości przy pomocy maszyny wytrzymałościowej (rys. 2). Otrzymane wyniki eksperymentalne potwierdziły, że pętle histerezy znacząco się zmieniają pod wpływem naprężeń.

Następnie wpływ naprężeń na pętle histerezy został zamodelowany przy użyciu rozszerzonego modelu Jilesa-Athertona na podstawie wyników z badań eksperymentalnych. Parametry modelu wyznaczono przy pomocy optymalizacji wieloparametrycznej, w której funkcja celu dana jest zależnością 13. Do minimalizacji zastosowano strategię ewolucyjną ($\mu + \lambda$) połączoną z symulowanym wyżarzaniem. Następnie 20 najlepszych zestawów paramentów modelu Jilesa-Athertona zostało poddanych optymalizacji gradientowej.

Wyniki modelowania z wykorzystaniem rozszerzonego modelu Jiles-Atherton są zgodne z wynikami pomiarów doświadczalnych dla pętli histerezy magnetycznej $B(H)$ (rys. 3, 4, 5). Zgodność wyników została potwierdzona za pomocą współczynnika determinacji R^2 , który przekroczył wartość 99% dla każdej pętli histerezy.